Translational Oncology 50 (2024) 102137

Contents lists available at ScienceDirect

Translational Oncology

journal homepage: www.elsevier.com/locate/tranon

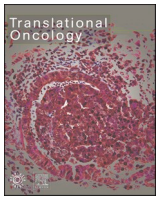

Original Research

Inhibition of hERG by ESEE suppresses the progression of colorectal cancer

Jufeng Wan [a,1], Haiying Xu [a,1], Jiaming Ju [d], Yingjie Chen [a], Hongxia Zhang [a], Lingling Qi [a], Yan Zhang [a,c], Zhimin Du [b,c,*], Xin Zhao [a,*]

[a] Department of Pharmacology, State Key Laboratory of Frigid Zone Cardiovascular Diseases (SKLFZCD) , (State Key Laboratory -Province Key Laboratories of Biomedicine-Pharmaceutics of China, Key Laboratory of Cardiovascular Research, Ministry of Education), College of Pharmacy, Harbin Medical University, Harbin 150081, China

[b] State Key Laboratory of Quality Research in Chinese Medicines, Macau University of Science and Technology, Macau 999078, China

[c] Institute of Clinical Pharmacy, the Second Affiliated Hospital, Harbin Medical University, Harbin, Heilongjiang 150081, China

[d] Translational Medicine Research and Cooperation Center of Northern China, Heilongjiang Academy of Medical Sciences, Harbin Medical University, Harbin, 150081, China

ARTICLE INFO

Keywords:
Emodin succinimidly ethyl esters
Colon cancer
hERG
FAK
Apoptosis

ABSTRACT

Colorectal cancer (CRC) is one of the most common malignant cancers. Emodin is a lipophilic anthraquinone commonly found in medicinal herbs and known for its antitumor properties. However, its clinical utility has been hampered by low druggability. We designed and synthesized a new compound named Emodin succinimidyl ethyl ester (ESEE), which improves the bioavailability and preserves the original pharmacological effects of Emodin. In vitro, we have confirmed that ESEE induces apoptosis in colon cancer cells, suppresses cell proliferation, migration, and invasion, and inhibits the growth of subcutaneous transplantation tumors associated with colon cancer. And, in vivo, ESEE robustly inhibited tumor growth. Human Ether-a-go-go Related Gene (hERG) is aberrantly expressed in various cancer cells, where they play an important role in cancer progression. Focal adhesion kinase (FAK) is a tyrosine kinase overexpressed in cancer cells and plays an important role in the progression of tumors to a malignant phenotype. Mechanistically, the anti-CRC properties of ESEE are exerted through direct binding with hERG, which impedes the FAK/PI3K/AKT signaling axis-dependent apoptotic cascade.

Introduction

CRC standing as the third most prevalent malignancy worldwide, resulted in 935,000 fatalities in 2020 [1-3]. At present, a variety of approaches are used in the clinical treatment of CRC, including traditional therapies such as surgery, chemotherapy, and radiotherapy, as well as newly emerging immunotherapeutic treatments and combination therapies [4]. Although these therapies have achieved clinical success, there are still many obstructing factors that affect the outcome of the treatment. drug resistance, hepatotoxicity and neurotoxicity [5-7]. Thus, there exists a pressing need to unveil innovative therapeutic paradigms and pharmacological agents to address these issues [8-11].

In recent years, with the advancement of modernizing traditional Chinese medicine, a plethora of natural small molecule compounds derived from traditional Chinese medicine have exhibited anti-tumor properties, including berberine, curcumin, and others [12-14]. Emodins, sourced from traditional Chinese medicinal herbs like rhubarb and cassia seed, have gained increasing attention [15,16]. Emodin demonstrates not only antibacterial, immunosuppressive, vasorelaxant, and anti-inflammatory effects but also has been evidenced to inhibit the progression of numerous cancers, including lung cancer and breast cancer [17-19]. Its multifaceted anti-tumor effects operate through diverse mechanisms. Emodin directly interacts with the transcriptional regulator Nuclear receptor corepressor 2 (NCOR2) , thereby promoting

Abbreviations: CRC, Colorectal cancer; ESEE, Emodin succinimidyl ethyl ester; hERG, Human Ether-a-go-go Related Gene; FAK, Focal adhesion kinase; PI3K, Phosphatidylinositol 3-kinase; AKT, V-akt murine thymoma viral oncogene homolog; NCOR2, Nuclear receptor corepressor 2; CCK-8, Cell Counting Kit-8; HT29, Human Colorectal Carcinoma Cells; IC50, 50 % inhibitory concentration; Ki-67, Proliferation cell nuclear antigen; DARTS, Drug Affinity Responsive Target Stability; CETSA, Cellular Thermal Shift Assay; Bax, BCL2 Associated X Protein; Bcl-2, B-cell lymphoma 2; TCM, Traditional Chinese medicine.

* Corresponding authors.
E-mail addresses: duzm@hrbmu.edu.cn (Z. Du), zhaoxin@hrbmu.edu.cn (X. Zhao).

[1] Jufeng Wan and Haiying Xu contributed equally to this work

https://doi.org/10.1016/j.tranon.2024.102137
Received 1 August 2024; Received in revised form 6 September 2024; Accepted 19 September 2024

the expression of SerRS and inhibiting angiogenesis via the VEGF signaling pathway, thereby attenuating the progression of triple-negative breast cancer [20]. Moreover, emodin exerts direct inhibitory effects on CRC progression by targeting VEGF [21,22]. Additionally, its efficacy extends to the induction of apoptosis and ferroptosis in tumor cells, highlighting its wide-ranging anticancer properties. Furthermore, emodin modulates the immune microenvironment by influencing macrophage function, consequently suppressing epithelial-mesenchymal transition and metastasis in breast cancer through the regulation of antitumor immunity. Significantly, emodin enhances the sensitivity of chemotherapy agents such as cisplatin and erythromycin, presenting a promising strategy to overcome tumor drug resistance.

Nevertheless, despite its potential, emodin is constrained by drawbacks such as hepatotoxicity, nephrotoxicity, reproductive toxicity, and low oral bioavailability, limiting its clinical utility [23,24]. Consequently, our team has developed a novel derivative of emodin - emodin succinyl ethyl ester (ESEE). Previous studies have indicated the superior pharmacokinetic properties of ESEE compared to emodin, characterized by lower Gibbs free energy and enhanced gastrointestinal absorption, making them promising candidates for drug development [25] However, the specific inhibitory effects of ESEE on colorectal cancer and its underlying mechanisms remain areas requiring comprehensive exploration and validation. Previous investigations have outlined the multifaceted therapeutic potential of ESEE, including the promotion of wound healing, attenuation of cardiac aging, mitigation of myocardial ischemia, and inhibition of hepatic lipid accumulation via diverse molecular pathways.

In this study, we elucidate the significant inhibitory effects of ESEE on the proliferative, migratory, and invasive abilities of CRC cells, as well as the suppression of xenograft tumor growth. Mechanistically, ESEE exerts its anti-CRC effects by directly binding to hERG, thereby hindering the apoptotic cascade dependent on the FAK/PI3K/AKT signaling axis.

Materials and methods

HT29 cell culture

Prepare frozen HT29 cell cryopreservation tubes from the liquid nitrogen tank and thaw them as quickly as possible in a 37 °C water bath. Aspirate the cell suspension into a centrifuge tube and add 10 times more culture medium, mix well. After centrifugation, the supernatant was discarded and added to 10 % serum culture medium inoculated into perforated culture flasks, and incubated at 37 °C under standard culture conditions. Passage culture was carried out according to the experimental plan.

CCK8 cell viability assay

The cell viability was detected by CCK8 kit. The HT29 cell suspension was inoculated into 96-well cell culture plate, the inoculation volume was 1×10^5 cells/ml, 100 μl per well, incubated at 37 °C for 24 h, then 100 μl of ESEE at each concentration was added, incubated at 37 °C for 24 h, after sufficient reaction, 10 μl of CCK8 was added to each well, incubate at 37 °C for one hour, protected from light, and the absorbance was measured by zymography at 450 nm.

Cell migration assay

The transwell chamber was placed in a 24-well culture plate, this chamber is called the upper chamber and the culture plate is called the lower chamber. HT29 cells were digested in serum-free medium, the cell density was adjusted to 5×10^5/ml, and the upper chamber was inoculated. Then 500 μl of serum-free culture medium, 5-FU, 10, 30, 100 μmol/L ESEE were added to the lower chamber to remove air bubbles between the upper and lower chambers. The culture was routinely incubated for 72 h. Cells were fixed with 4 % paraformaldehyde and washed with PBS. Then the cells were stained with 0.1 % crystal violet, and representative images were observed by light microscope.

Cell invasion assay

The Transwell invasion assay was performed by pre-coating the upper membrane with 100 μl of matrix gel, encapsulating the bottom membrane of the chambers, and leaving it in the incubator at 37 °C for 1 h to polymerize the gel. HT29 cells were taken to adjust the cell density to 5×10^5/ml. The upper chamber was inoculated, and 500 μl of serum-free culture medium, 5-FU, 10, 30, and 100 μmol/L ESEE were added to the lower chamber to remove air bubbles between the upper and lower chambers, respectively. Cells were fixed with 4 % paraformaldehyde and washed with PBS. Then the cells were stained with 0.1 % crystal violet, and representative images were observed by light microscope.

3D invasion experiment

Pre-cool the yellow lance tip, 1.5 ml EP tube, and ice plate in advance, and thaw the matrix gel. The cell concentration was adjusted to 5×10^4 cells/ml, 200 μl of cell suspension per well was inoculated into 96-well U-plates, and after 72 h of incubation, 3D cell spheres were viewed under the microscope, 100 μl of supernatant in the plate was discarded, and 100 μl of rhamnogelinogen and matrix gel were prepared according to the ratio of 1:1 for each well, and then the plate was placed in the incubator and cured for one hour, and then taken out, 100 μl of serum-free culture medium, 5-FU, 10, 30, 100 μmol/L ESEE was added into each well, and the plate was thawed under the microscope. After curing in the incubator for 1 hour, 100 μl of serum-free culture medium, 5-FU, 10, 30, and 100 μmol/L ESEE were added to each well, and pictures were taken under the microscope.

AnnexinV-FITC/PI combined with flow cytometry

HT29 cells treated with drugs for 24 h are collected directly in centrifuge tubes. After centrifugation, the cells are washed once with PBS buffer and centrifuged at 1000 rpm for 5 min. 1 ml of deionized water and 3 ml of binding buffer were used to resuspend the cells to the desired concentration. Incubate the sample with a mixture of Annexin V-FITC and PI for 15 min at room temperature. Detection should be performed via flow cytometry.

Ki67 staining

HT29 cells were incubated with serum-free culture medium, 5-FU, 10, 30, and 100 μmol/LESEE added to each well after 24 h of inoculation on glass bottom plates. The plates were fixed with 4 % paraformaldehyde for 30 min and permeabilized with permeabilizing solution for 20 min. After blocking with 5 % BSA for 45 min, incubation with Ki67 antibody was performed at 4 °C overnight. Samples were washed three times with PBS for 5 min between each step. Immunofluorescent secondary antibodies were incubated at room temperature for 1 hour and photographed under a fluorescence microscope.

Immunoblotting assay

Cells or tissues were collected and added to RIPA protein lysate buffer for protein extraction and protein concentration was determined using the BCA protein quantification kit. After electrophoresis on SDS-PAGE (10 %), membrane transfer, closure, and TBST washing, incubate primary antibody overnight at 4 °C. The primary antibodies were incubated with:hERG (1:500, Santa Cruz), FAK(1:1000,Cell Signaling Technology),p-FAK Tyr397(1:500, Santa Cruz),PI3K p85 (1:1000, Cell Signaling Technology),AKT (1:1000, Cell Signaling Technology), p-AKT

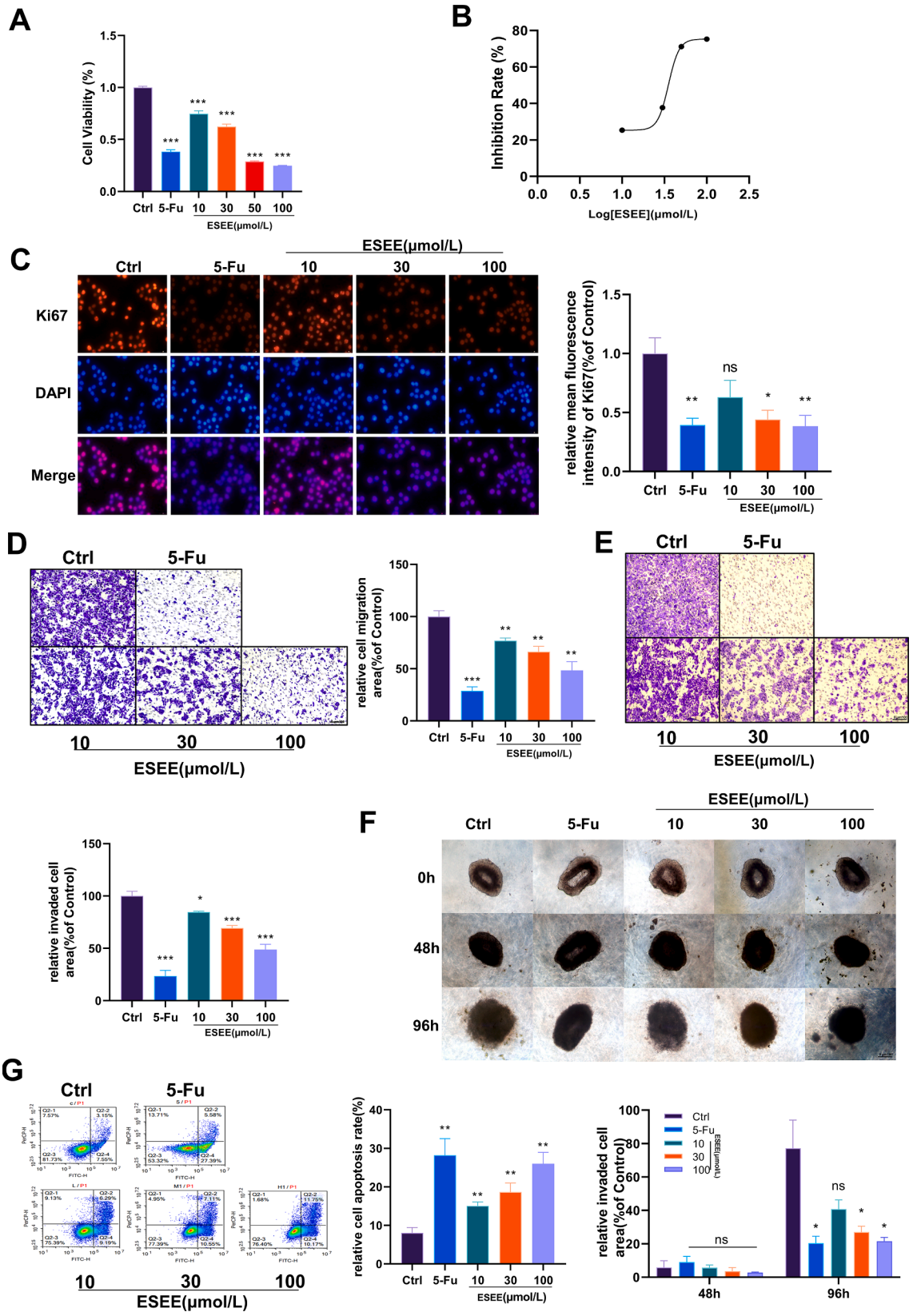

Fig. 1. ESEE affects the growth of colon cancer cells. (A) Results of HT29 cell activity. (B) The effect of ESEE inhibiting HT29 cell viability. (C) Results of Ki67 fluorescence intensity of HT29 cells. Comparison of positive rates of KI67 in the control,5-FU, ESEE: 10, 30, and 100 umol/L groups. (D) Migration results of HT29 cells treated with 5-Fu or 10,30,100 μM ESEE. The relative cell migration areas of the five groups were counted. (E)Results of Transwell assay of HT29 cells treated with 5-Fu or 10,30,100 μM ESEE.The relative cell invasion areas of the five groups were counted. (F)Results of 3D invasion experiment of HT29 cells treated with 5-Fu or 10,30,100 μM ESEE for 0,48 or 96 h. (G) Results of flow cytometry of HT29 cells treated with 5-Fu or 10,30,100 μM ESEE. The percentage of apoptotic cells in the different treatment groups was counted to reflect the rate of apoptosis in different treatment situations. Images were displayed at magnification of 40 × or 20 × . Statistical significance was assessed by One-way ANOVA. Graphs display mean±SEM (n.s. * $P < 0.05$,** $P < 0.01$,*** $P < 0.001$ vs. Control, $n = 4$).

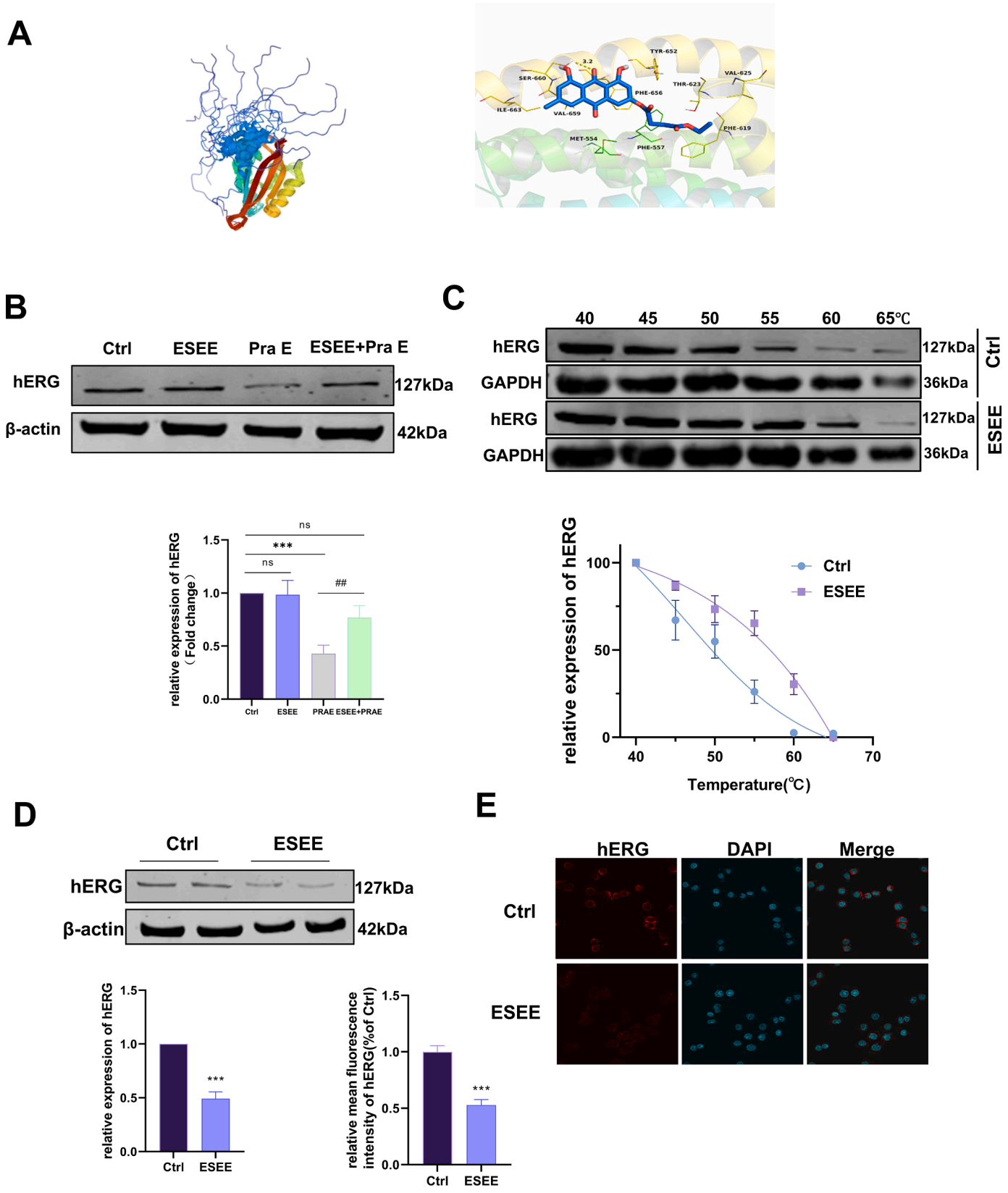

Fig. 2. ESEE inhibits colon cancer cell growth by directly binding the hERG channel. (A) 3D structure of hERG and the ESEE was docked into the binding site of the hERG. (B) ESEE was incubated with cell lysate, and after the enzymolysis experiment, the expression of the hERG channel in HT29 cells of each group was analyzed by gel electrophoresis. β-actin served as the internal control. (C) HT29 cells were exposed for 2 h to DMSO or 100 μmol/L ESEE and subject to CETSA. The intensity of the hERG bands was quantified to exhibit the binding affinity of ESEE to hERG in HT29 cells. GAPDH served as the internal control. (D) Gel electrophoresis of hERG channel expression in HT29 cells in Control group and 100μmol/L ESEE group. β-actin served as the internal control. (E) Immunofluorescence of hERG channel. The alterations in hERG fluorescence intensity were observed following ESEE treatment. Images were displayed at a magnification of 60 × . Statistical significance was assessed by One-way ANOVA. Graphs display mean±SEM (n.s. *** $P < 0.001$ vs. Control, ## $P < 0.01$ vs. PRAE, $n = 4$).

Ser473 (1:2000, Cell Signaling Technology), Bcl-2 (1:1000, Cell Signaling Technology), Bcl-2 (1:1000, Cell Signaling Technology). The secondary antibody was incubated for 50 min the next day. The membrane was scanned and the protein bands were analyzed by Odyssey Infrared Fluorescence Scanning System.

Animal experimental methods

Take HT29 cells and digest the cells, adjust the cell density to 1×10^7 cells/ml, and make cell suspension. HT29 cells were injected subcutaneously into the back of nude mice, and 0.2 ml was injected into each mouse. Grouping and administration of experimental animals: after tumor modeling, nude mice were randomly grouped into tumor model group, 5-FU group, 180 mg kg^{-1} emodin group, 20, 60, 180 mg kg^{-1} ESEE group, and 12 mice in each group. 5-FU was injected intraperitoneally every two days, and ESEE and emodin were administered by gastric gavage every day for a total of 28 days, to observe the tumor formation and survival. Tumor formation and survival were observed. 28 days after drug administration, mice were executed, tumor tissues were removed, weighed and measured for volume, and photographed.

Immunofluorescence

HT29 cells were inoculated on confocal dishes for 24 h and incubated with serum-free culture medium and 100 μmol/LESEE added separately. HT29 cells were fixed for 30 min and permeabilized with immunofluorescence permeabilization solution for 20 min. BSA was used to confine the cells at room temperature for 45 min before incubating with primary antibody at 4 °Covernight. Wash with PBS between each step. Fluorescent secondary antibodies were incubated for 1 h at room temperature, incubated with DAPI for 50 s, and photographed by laser confocal.

Drug target affinity stability assay (DARTS)

The M-PRE extract was added to the HT29 cells in good growth condition and then scraped into the EP tube with a spatula for centrifugation, the supernatant was taken and the protein concentration was measured by the BCA Protein Assay Kit. The protein samples were divided into four groups: (1) Control group; (2) ESEE group; (3) Streptavidin group; and (4) ESEE+Streptavidin group. The protein samples were incubated with DMSO and 100 μmol/L ESEE for 1 hour at room temperature. Then, add the corresponding amount of streptavidin (streptavidin concentration 10 mg/ml) to the protein samples, incubate for 20 min at room temperature, and add SDS-PAGE protein sample buffer to terminate the enzymatic reaction. hERG channel expression was analyzed by Western Blot.

Molecular docking

Molecular docking technique was utilized to verify the interaction between ESEE and hERG protein. Firstly, receptor preparation was carried out. After the crystal structure of hERG channel was obtained from PDB database (https: //www.rcsb.org/), the receptor was preprocessed using PyMOL software. Next, ligand preparation was carried out. The chemical structure of ESEE was drawn using Chem Office software to generate small molecule ligands. After that, we used Auto Grid program to generate the receptor grid, set the algorithm and docking parameters, docked the hERG channel with ESEE using Auto Dock software, tested the docking energy reasonableness, screened out the drug-target binding models with high scores, and optimized the conditions to improve the docking efficiency and accuracy for the subsequent experiments.

Cellular thermal migration analysis (CETSA)

Cellular thermal displacement assay was used to detect the binding of ESEE to hERG. Full-grown HT29 cells were taken and lysed with appropriate amount of RIPA lysate, cell lysates were collected and centrifuged, then DMSO and 100 μmol/L ESEE were added and incubated for 2 h at room temperature. The cell lysate was divided into six equal portions and heated at 40, 45, 50, 55, 60, and 65 °C for 3 min, and the heated protein samples were centrifuged at 20,000 g for 15 min, and the supernatant was collected and added into SDS-PAGESDS-PAGE protein sample buffer. hERG channel expression was analyzed by Western Blot.

Statistical analysis

Data were analyzed using Graphpad PrismPrism 8.3.0 software. Data were expressed as mean ± standard error (mean ± SEM). Two samples were tested using independent samples *t*-test. $P < 0.05$ indicates that the difference between groups is statistically significant, $P < 0.01$ indicates that the difference between groups is statistically significant, and $P < 0.001$ indicates that the difference between groups is statistically highly significant.

Results

ESEE inhibits the growth and induces apoptosis in HT29 cells

In order to assess the effect of ESEE on human CRC cells, CCK-8 assay was performed. Human CRC cell line HT29 cells were treated with various concentrations of ESEE for 24 h, The results revealed that ESEE inhibited human CRC cell growth in dose-dependent manners. Furthermore, the IC50 value of ESEE on HT29 cells was determined to be [values](Fig. 1A-B). The positive rate of Ki-67, a marker of cell proliferation, decreased with increasing doses of ESEE, suggesting an impairment in the proliferation ability of HT29 cells(Fig. 1C). The Transwell experiment demonstrated that ESEE also suppresses the migration and invasion capabilities of HT29 cells in a dose-dependent manner(Fig. 1D-E). Furthermore, we conducted 3D invasion experiments using HT29 cell spheres, and the results indicated that ESEE incubation significantly inhibited the invasion of tumor spheres into the surrounding matrix(Fig. 1F). In order to detect the inhibitory mechanism of ESEE on HT29 cells, apoptosis, an important type of programmed cell death, was detected by Annexin V /PI double staining (Fig. 1G). As depicted in Fig. 1A ,B, ESEE dose-dependently induced apoptosis in HT29 cells. These findings collectively demonstrate that ESEE inhibits CRC cell proliferation, migration, and invasion while inducing apoptosis.

ESEE directly binds with hERG

To elucidate the molecular mechanism by which ESEE inhibits CRC, we identified hERG as the direct target of ESEE through molecular docking experiments(Fig. 2A). It has been reported that the hERG channel protein is highly expressed in colon cancer, and this channel can facilitate the progression of colorectal cancer through various signaling pathways [26]. Therefore, we hypothesize that ESEE may exert anti-colorectal cancer effects by targeting the hERG channel.

ESEE was docked into the binding site of the hERG and the result was shown in Fig. 2A. The maximum binding affinity between ESEE and the hERG was predicted to be −5.7 kcal/mol. ESEE adopted a compact conformation to bind at the surface of the hERG. Detailed analysis showed that the ESEE stretched into the hydrophobic pocket that consisted of the residues Met-554, Phe-557, Phe-619, Val-625, Phe-656, Val-659, and Ile-663 forming a strong hydrophobic binding. In addition, the anthraquinone scaffold of the ESEE formed the π-π stacking interaction with the residue Phe-656. Importantly, one key hydrogen bond interaction was observed between one of the methoxyl groups of ESEE and the residue Ser-660, with the bond length of 3.2 Å, which was the main interaction between the ESEE and the hERG. All these

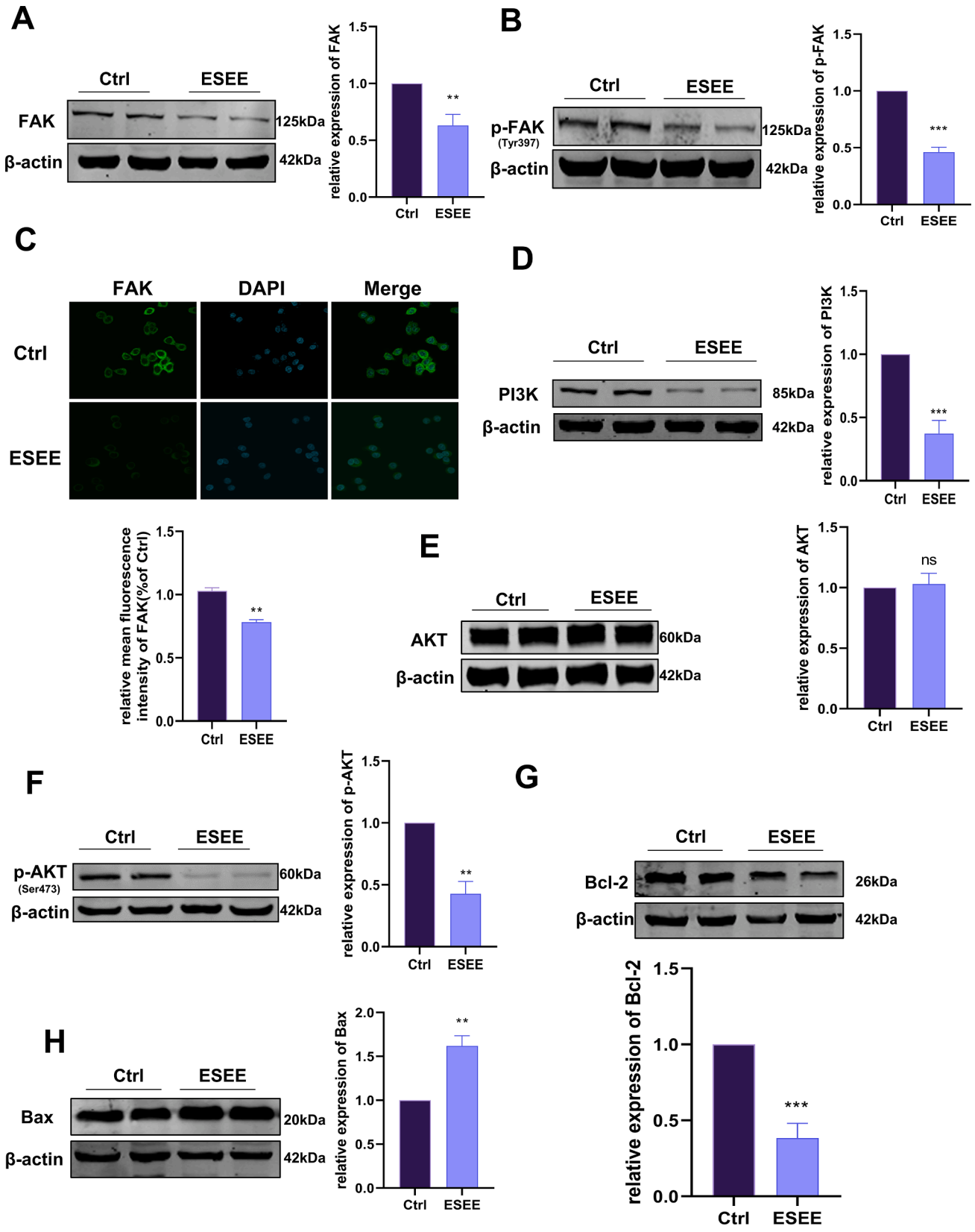

Fig. 3. ESEE affects the expression of FAK, PI3K, AKT, Bcl-2, and Bax proteins in colon cancer cells. The protein expression levels of FAK, p-FAK, PI3K, AKT, p-AKT, Bcl-2, and Bax were assessed following treatment with 100μmol/L ESEE in cells. (A) Gel electrophoresis of FAK protein expression in HT29 cells in Control group and 100 μmol/L ESEE group. β-actin served as the internal control. (B) Gel electrophoresis of p-FAK protein expression in HT29 cells. (C) Immunofluorescence of FAK protein expression. Immunofluorescence statistics of changes in FAK fluorescence intensity after ESEE treatment. (D) Gel electrophoresis of PI3K protein expression. (E) Gel electrophoresis of AKT protein expression. (F) Gel electrophoresis of p-AKT protein expression. (G) Gel electrophoresis of Bcl-2 protein expression. (H) Gel electrophoresis of Bax protein expression. β-actin served as the internal control. Images were displayed at a magnification of 60 × . Statistical significance was assessed by One-way ANOVA. Graphs display mean±SEM (n.s.** $P < 0.01$, *** $P < 0.001$ vs. Control, $n = 4$).

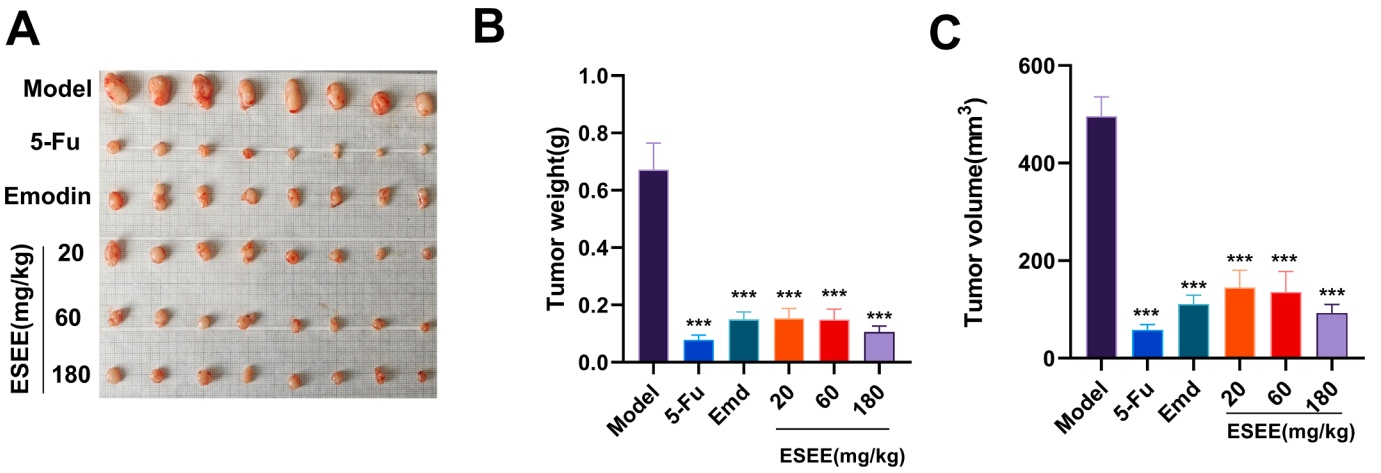

Fig. 4. ESEE can reduce tumor volume and weight in model mice. (A) Results of colon cancer tissue after sampling. (B) Statistical chart of colon cancer tissue weight. (C) Statistical chart of colon cancer tissue volume(Length*Width squared/2). Statistical significance was assessed by One-way ANOVA. Graphs display mean±SEM (n. s. $^{***}P < 0.001$ vs. Model, $n = 8$).

interactions helped ESEE to anchor in the binding site of hERG.

To further confirm whether ESEE can directly bind to hERG, we conducted Drug Affinity Response Target Stability (DARTS) and Cellular Thermal Shift Assay (CETSA). The CETSA indicated that the incubation of ESEE enhances the resistance of hERG protein against hydrolysis, suggesting that ESEE improves the stability of hERG(Fig. 2B). DARTS suggested that treatment with ESEE resulted in a rightward shift in the hERG melting curve, suggesting increased thermal stability and direct binding of ESEE to hERG proteins(Fig. 2C). Furthermore, following a 24-hour incubation with ESEE, the protein expression of hERG in HT29 cells significantly decreased(Fig. 2D). Immuno-fluorescence experiments also revealed a significant reduction in the accumulation of hERG protein on the cell membrane in HT29 cells incubated with ESEE(Fig. 2E). Therefore, the results suggest that ESEE may directly target hERG and inhibit the progression of CRC.

ESEE inhibits hERG-mediated PI3K/AKT in HT29 cells

It is found that hERG channel modulates the expression and activation of focal adhesion kinase (FAK) in CRC, with hERG channel expression positively correlated with FAK protein levels. Immunoblotting suggested that the expression of FAK and p-FAK proteins was notably diminished after ESEE administration (Fig. 3A-B). Moreover, immunofluorescence also indicated that administering ESEE to HT29 cells can reduce the fluorescence intensity of FAK (Fig. 3C). These results collectively suggest that ESEE possesses the ability to suppress the expression and phosphorylation of FAK. Notably, FAK can trigger downstream signaling cascades by influencing phosphoinositide 3-kinase (PI3K) expression, thereby orchestrating critical cellular processes such as proliferation, migration, invasion, and adhesion. Our findings indicate the protein level of PI3K was significantly reduced in the ESEE administration, indicating the inhibitory effect of ESEE on PI3K protein (Fig. 3D). In addition, no considerable alterations were observed in AKT protein levels, while markedly lower levels of p-AKT were detected after ESEE administration(Fig. 3E-F). Notably, the protein level of Bcl-2 experienced a significant reduction, whereas the level of Bax was elevated after ESEE administration (Fig. 3G-H). Overall, the results indicate that ESEE can target the hERG-mediated PI3K/AKT signaling pathway to induce HT29 cell apoptosis.

ESEE inhibits the growth of CRC xenograft tumors

To assess the effect of ESEE on tumor growth in animal models, a xenograft model was established. After 28 days of oral administration of ESEE, tumor tissues were extracted and evaluated for volume and weight(Fig. 4A-C). Therefore, these results indicate that ESEE has the potential to inhibit the progression of CRC.

ESEE inhibited CRC progression via hERG/FAK/PI3K/AKT signaling

To investigate the effect of ESEE on hERG and related proteins in xenograft tumor tissues, we measured the relative content of hERG, FAK, PI3K, AKT, Bax, and Bcl-2. The results showed that the expression of hERG in tumor tissues treated with ESEE was significantly inhibited, and the fluorescence intensity of hERG was also significantly reduced (Fig. 5A-J). Hence, the findings suggest that ESEE modulates the hERG/FAK/PI3K/AKT-mediated cell apoptosis pathway, thereby suppressing the progression of colorectal cancer.

Discussion

CRC has high incidence rates, frequent postoperative recurrences, and a high mortality rate since colon cancer is a common malignant tumor of the digestive tract. However, treatments for CRC are currently limited and often have adverse effects, making them prone to recurrence [27]. Therefore, there is a need to develop alternative therapies. Currently, TCM plays an important role in the adjuvant treatment of tumor radiotherapy and chemotherapy, and the synergistic detoxification effect of TCM is more and more recognized [28-32]. ESEE is a novel drug developed by our team, which improves bioavailability and reduces toxicity by modifying the natural drug Emodin. Studies have already shown that ESEE has a lower Gibbs free energy than Emodin and has a higher success rate as a drug. In this study, we demonstrated the ability of ESEE to inhibit tumor growth, reduce tumor size, and decrease tumor weight compared to the model group using a subcutaneous graft tumor model of colon cancer. These results suggest that ESEE may be a potential alternative to current chemotherapeutic agents due to its lower toxicity, higher safety index, and ability to halt colon cancer progression. Taken together, these data suggest that ESEE is a promising chemotherapeutic agent for CRC and is a therapeutic candidate due to its superior efficacy and safety profile. The development and clinical translation of ESEE may provide a more effective and safer therapeutic option for colon cancer patients. However, there is no research report regarding the specific mechanism of ESEE inhibition of colon cancer progression, therefore, our group investigated the specific mechanism of ESEE inhibition of colon cancer progression. We focused our attention on hERG channels, which are closely related to colon cancer, based on previous studies.

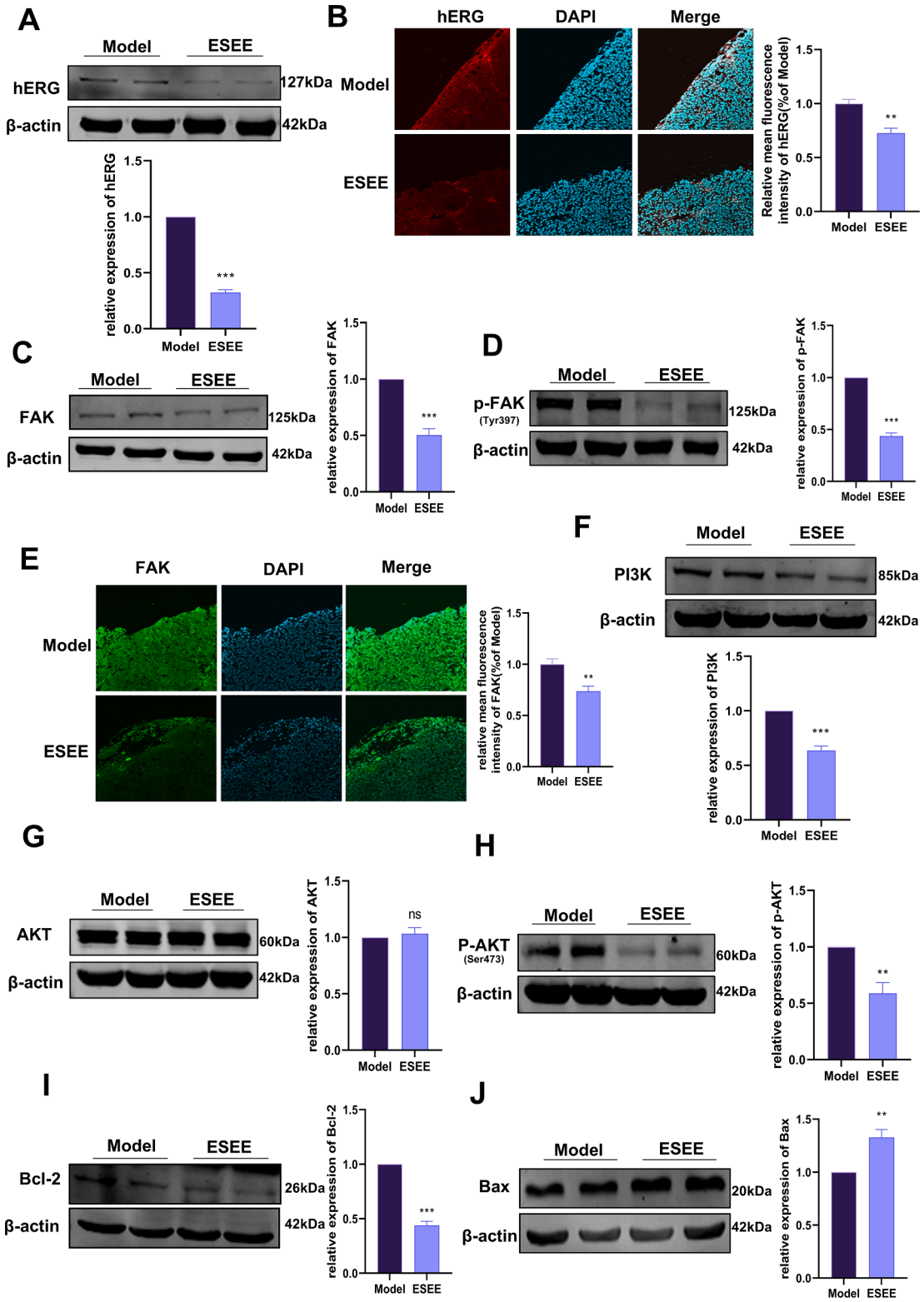

Fig. 5. ESEE inhibits the expression of the hERG-FAK-PI3K-AKT signaling pathway in colon cancer transplant tumors. The protein expression levels of hERG, FAK, p-FAK, PI3K, AKT, p-AKT, Bcl-2, and Bax were assessed following treatment with 100μmol/L ESEE in tumors. (A) Gel electrophoresis of hERG channel expression in Model group and 180 mg kg^{-1} ESEE group in colon cancer transplant tumors. (B) Immunofluorescence of hERG channel in colon cancer transplant tumors. Immunofluorescence statistics of changes in hERG fluorescence intensity after ESEE treatment. (C) Gel electrophoresis of FAK protein expression. (D) Gel electrophoresis of p-FAK protein expression in Model group and 180 mg kg^{-1} ESEE group in colon cancer transplant tumors. (E) Immunofluorescence of FAK channel. Immunofluorescence statistics of changes in FAK fluorescence intensity after ESEE treatment. (F) Gel electrophoresis of PI3K protein expression. (G) Gel electrophoresis of AKT protein expression. (H) Gel electrophoresis of p-AKT protein expression. (I) Gel electrophoresis of Bcl-2 protein expression. (J) Gel electrophoresis of Bax protein expression. β-actin served as the internal control. Images were displayed at a magnification of 20 × . Statistical significance was assessed by One-way ANOVA. Graphs display mean±SEM (n.s.** $P < 0.01$, *** $P < 0.001$ vs. Model, $n = 4$).

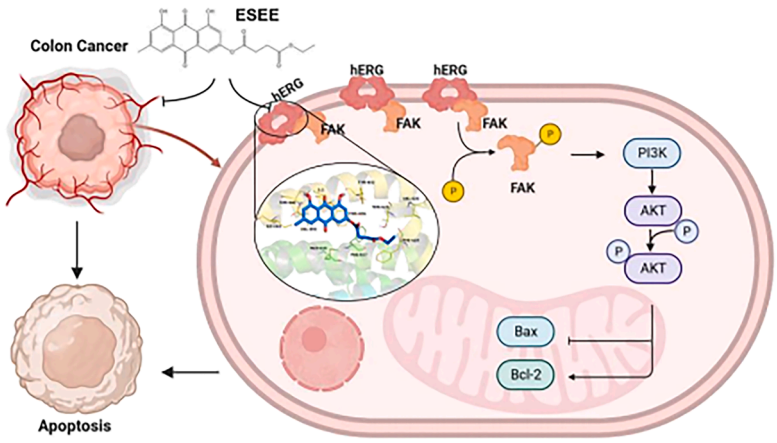

Fig. 6. The mechanism of action of ESEE against colon cancer: ESEE promotes apoptosis and inhibits the development of colon cancer by regulating hERG pathway and then inhibiting FAK-PI3K-AKT pathway.

The hERG is a voltage-gated K^+ channel that is physiologically expressed in cardiomyocytes, neurons, smooth muscle, and neuroendocrine cells of various organs [33]. There is evidence that hERG is aberrantly expressed in various cancer cells and plays an important role in CRC progression. Therefore, hERG may be a potential biomarker for cancer and a potential molecular target for anticancer drug development [34]. Previously, it has been reported that inhibition of hERG expression in tumor cells can exert antitumor effects, but the specific mechanism has rarely been investigated. A detailed analysis revealed that ESEE binds directly to hERG, extending into a hydrophobic pocket consisting of Met-554, Phe-557, Phe-619, Val-625, Phe-656, Val-659, and Ile-663, forming a strong hydrophobic binding. Additionally, the anthraquinone scaffold of ESEE engages in a π-π stacking interaction with residue Phe-656. It is of particular significance that a pivotal hydrogen bonding interaction with a bond length of 3.2 Å was observed between a methoxy group of ESEE and residue Ser-660, which represents the primary interaction between ESEE and hERG. These interactions collectively facilitate the anchoring of ESEE to the binding site of hERG.

Conformational changes in the voltage-gated structural domains of hERG channels can directly interact with integrin β1 and FAK in lipid rafts to promote cell migration, which is a key factor in cancer metastasis. The non-receptor protein tyrosine kinase, p-FAK, plays a crucial role in various cellular processes, including cell proliferation, migration, invasion, and adhesion [35]. The study found that levels of FAK and p-FAK proteins decreased in CRC cells and tumor tissues after ESEE treatment. This suggests that inhibiting CRC may be associated with changes in FAK expression. Previous reports have shown that the FAK pathway can activate PI3K and its downstream effectors to regulate tumor cells. Therefore, we further investigated the PI3K pathway [36, 37]. The results of this study demonstrate that ESEE inhibits colon cancer development by suppressing PI3K protein levels, down-regulating phosphorylated AKT levels, and consequently inhibiting AKT activation [38]. Apoptosis, a form of programmed cell death, is a promising target for anticancer therapies because it is a highly selective process that is critical under both physiological and pathological conditions. Proteins that regulate apoptosis include two major classes: pro-apoptotic proteins (such as Bax and Bak) and anti-apoptotic proteins (such as Bcl-2 and Bcl-XL) [39,40]. Anti-apoptotic proteins inhibit the release of cytochrome c from mitochondria, while pro-apoptotic proteins promote its release. The Western blotting results showed that ESEE administration increased Bax expression levels, and decreased Bcl-2 expression levels, leading to Bcl-2 interaction with Bax and apoptosis promotion.

In conclusion, the results demonstrated that ESEE inhibited hERG and promoted FAK phosphorylation, thereby regulating the downstream PI3K/AKT signaling pathway to play an anticancer role by inhibiting the proliferation, migration, and inducing apoptosis of CRC cells. (Fig. 6). This study deepens our understanding of the anticancer properties of ESEE and lays the foundation for its clinical application in the treatment of CRC. This research extends our understanding of the anticancer effects of ESEE and demonstrates its potential for application in the treatment of CRC. The major limitations of the present study is that don't provide a comprehensive analysis of the precise mechanism by which ESEE induces a reduction in hERG expression. Future research should be undertaken to explore the specific mechanisms of ESEE reduction of hERG expression. In the next five years, it is expected that the function of traditional Chinese medicine and its derivatives in colorectal cancer will continue to be discovered. ESEE will provide clinicians with more combination therapy approaches in the treatment of colon cancer.

CRediT authorship contribution statement

Jufeng Wan: Writing – review & editing, Writing – original draft, Validation, Supervision, Project administration, Formal analysis, Data curation. **Haiying Xu:** Validation, Supervision, Software, Investigation, Data curation. **Jiaming Ju:** Investigation. **Yingjie Chen:** Writing – original draft, Validation, Project administration, Investigation. **Hongxia Zhang:** Validation, Investigation, Data curation. **Lingling Qi:** Investigation, Data curation. **Yan Zhang:** Writing – review & editing, Visualization, Project administration, Methodology, Formal analysis. **Zhimin Du:** Writing – review & editing, Supervision, Resources, Conceptualization. **Xin Zhao:** Writing – review & editing, Visualization, Software, Methodology, Funding acquisition, Conceptualization.

Declaration of competing interest

The authors declare that they have no known competing financial interests or personal relationships that could have appeared to influence the work reported in this paper.

References

[1] R.L. Siegel, A.N. Giaquinto, A. Jemal, Cancer statistics, 2024, CA Cancer J. Clin. 74 (1) (2024) 12–49.
[2] L. DeDecker, et al., Microbiome distinctions between the CRC carcinogenic pathways, Gut. Microbes. 13 (1) (2021) 1854641.
[3] X. Chen, et al., Chalcone Derivative CX258 Suppresses Colorectal Cancer via Inhibiting the TOP2A/Wnt/β-Catenin Signaling, Cells (7) (2023) 12.
[4] Y. Liu, et al., GPC1 Is Associated with Poor Prognosis and Treg Infiltration in Colon Adenocarcinoma, Comput. Math. Methods Med. 2022 (2022) 8209700.
[5] G. Brandi, et al., Is post-transplant chemotherapy feasible in liver transplantation for colorectal cancer liver metastases? Cancer Commun. (Lond) 40 (9) (2020) 461–464.
[6] D. Basak, M.N. Uddin, J. Hancock, The Role of Oxidative Stress and Its Counteractive Utility in Colorectal Cancer (CRC), Cancers. (Basel) 12 (11) (2020).

[7] A. Rizzo, et al., Peripheral neuropathy and headache in cancer patients treated with immunotherapy and immuno-oncology combinations: the MOUSEION-02 study, Expert. Opin. Drug Metab. Toxicol. 17 (12) (2022) 1455–1466.
[8] P. Lamichhane, et al., Colorectal Cancer and Probiotics: are Bugs Really Drugs? Cancers. (Basel) 12 (5) (2020).
[9] B. Suo, C. Wu, F. Mei, Effect of bevacizumab on expression level of GLI1 and ING4 in colon cancer animal model, Oncol. Lett. 20 (2) (2020) 1263–1269.
[10] W. Sun, et al., *Lnc HAGLR Promotes Colon Cancer Progression Through Sponging miR-185-5p and Activating CDK4 and CDK6* in vitro *and* in vivo, Onco Targets. Ther. 13 (2020) 5913–5925.
[11] L. Ng, et al., Repurposing DPP-4 Inhibitors for Colorectal Cancer: a Retrospective and Single Center Study, Cancers. (Basel) 13 (14) (2021).
[12] J.W. Zhang, et al., Anti-Tumor Effects of Paeoniflorin on Epithelial-To-Mesenchymal Transition in Human Colorectal Cancer Cells, Med. Sci. Monit. 24 (2018) 6405–6413.
[13] G. Lu, et al., Deguelin Attenuates Non-Small-Cell Lung Cancer Cell Metastasis by Upregulating PTEN/KLF4/EMT Signaling Pathway, Dis. Markers 2022 (2022) 4090346.
[14] S. Hong, et al., Ginsenoside Rg3 enhances the anticancer effect of 5-FU in colon cancer cells via the PI3K/AKT pathway, Oncol. Rep. 44 (4) (2020) 1333–1342.
[15] Q. Li, et al., Molecular Mechanisms of Action of Emodin: as an Anti-Cardiovascular Disease Drug, Front. Pharmacol. 11 (2020) 559607.
[16] R.B. Semwal, et al., *Emodin - A natural anthraquinone derivative with diverse pharmacological activities*, Phytochemistry (2021) 190.
[17] Y. Song, et al., Ferrimagnetic mPEG-b-PHEP copolymer micelles loaded with iron oxide nanocubes and emodin for enhanced magnetic hyperthermia-chemotherapy, Natl. Sci. Rev. 7 (4) (2020) 723–736.
[18] Q. Zhang, et al., The versatile emodin: a natural easily acquired anthraquinone possesses promising anticancer properties against a variety of cancers, Int. J. Biol. Sci. 18 (8) (2022) 3498–3527.
[19] G. Dai, et al., ACSL4 promotes colorectal cancer and is a potential therapeutic target of emodin, Phytomedicine 102 (2022) 154149.
[20] G. Zou, et al., Herb-sourced emodin inhibits angiogenesis of breast cancer by targeting VEGFA transcription, Theranostics. 10 (15) (2020) 6839–6853.
[21] Y. Lu, J. Zhang, J. Qian, The effect of emodin on VEGF receptors in human colon cancer cells, Cancer BiOther Radiopharm. 23 (2) (2008) 222–228.
[22] G. Dai, et al., Emodin suppresses growth and invasion of colorectal cancer cells by inhibiting VEGFR2, Eur. J. Pharmacol. 859 (2019) 172525.
[23] S.J. McDonald, et al., Therapeutic Potential of Emodin for Gastrointestinal Cancers, Integr. Cancer Ther. 21 (2022).
[24] C. Chen, et al., NMR-based Metabolomic Techniques Identify the Toxicity of Emodin in HepG2 Cells, Sci. Rep. 8 (1) (2018) 9379.
[25] X. Liu, et al., Kanglexin protects against cardiac fibrosis and dysfunction in mice by TGF-β1/ERK1/2 noncanonical pathway, Front. Pharmacol. 11 (2020) 572637.
[26] D. Sacks, et al., Multisociety Consensus Quality Improvement Revised Consensus Statement for Endovascular Therapy of Acute Ischemic Stroke, Int. J. Stroke 13 (6) (2018) 612–632.
[27] P. Shayimu, et al., MTBP promoted the proliferation, migration and invasion of colon cancer cells by activating the expression of ZEB2, Anim. Cells Syst. (Seoul) 25 (3) (2021) 152–160.
[28] J. Huang, et al., Characterization of the mechanism of Scutellaria baicalensis on reversing radio-resistance in colorectal cancer, Transl. Oncol. 24 (2022) 101488.
[29] K. Wang, et al., Anticancer activities of TCM and their active components against tumor metastasis, Biomed. Pharmacother. 133 (2021).
[30] Y. Liu, et al., Cellular senescence and cancer: focusing on traditional Chinese medicine and natural products, Cell Prolif. 53 (10) (2020).
[31] Z. Wei, et al., Traditional Chinese Medicine has great potential as candidate drugs for lung cancer: a review, J. Ethnopharmacol. 300 (2023).
[32] S. Wang, et al., Metabolic reprogramming by traditional Chinese medicine and its role in effective cancer therapy, Pharmacol. Res. 170 (2021).
[33] B.J. Zünkler, Multiple hERG channel blocking pathways: implications for macromolecules, Trends Pharmacol. Sci. 45 (8) (2024) 671–677.
[34] S. He, et al., HERG channel and cancer: a mechanistic review of carcinogenic processes and therapeutic potential, Biochim. Biophys. Acta Rev. Cancer 1873 (2) (2020) 188355.
[35] J.T. Parsons, Focal adhesion kinase: the first ten years, J. Cell Sci. 116 (Pt 8) (2003) 1409–1416.
[36] J. Luo, B.D. Manning, L.C. Cantley, Targeting the PI3K-Akt pathway in human cancer: rationale and promise, Cancer Cell 4 (4) (2003) 257–262.
[37] K.K. Wong, J.A. Engelman, L.C. Cantley, Targeting the PI3K signaling pathway in cancer, Curr. Opin. Genet. Dev. 20 (1) (2010) 87–90.
[38] Y. Yue, et al., Upregulated expression levels of ADAM10 and EGFR and downregulated expression levels of E-cadherin in hepatocellular carcinomas, Exp. Ther. Med. 6 (6) (2013) 1380–1384.
[39] B. Liu, et al., Livin/ML-IAP as a new target for cancer treatment, Cancer Lett. 250 (2) (2007) 168–176.
[40] A. Ashkenazi, et al., From basic apoptosis discoveries to advanced selective BCL-2 family inhibitors, Nat. Rev. Drug Discov. 16 (4) (2017) 273–284.